Published in final edited form as:
Eur J Neurosci. 2008 August ; 28(3): 510–520. doi:10.1111/j.1460-9568.2008.06345.x.

Brain-derived neurotrophic factor enhances fetal respiratory rhythm frequency in the mouse preBötzinger complex *in vitro*

Julien Bouvier[1], **Sandra Autran**[1], **Nathalie Dehorter**[1,*], **David M. Katz**[2], **Jean Champagnat**[1], **Gilles Fortin**[1], and **Muriel Thoby-Brisson**[1]

1 *Laboratoire de Neurobiologie Génétique et Intégrative (NGI), Institut Alfred Fessard, Centre National de la Recherche Scientifique, 91198 Gif sur Yvette, France*

2 *Department of Neurosciences, School of Medicine, Case Western Reserve University, Cleveland, OH, USA*

Abstract

Brain-derived neurotrophic factor (BDNF) is required during the prenatal period for normal development of the respiratory central command; however, the underlying mechanisms remain unknown. To approach this issue, the present study examined BDNF regulation of fetal respiratory rhythm generation in the preBötzinger complex (preBötC) of the mouse, using transverse brainstem slices obtained from prenatal day 16.5 animals. BDNF application (100 ng/mL, 15 min) increased the frequency of rhythmic population activity in the preBötC by 43%. This effect was not observed when preparations were exposed to nerve growth factor (100 ng/mL, 30 min) or pretreated with the tyrosine kinase inhibitor K252a (1 h, 200 nM), suggesting that BDNF regulation of preBötC activity requires activation of its cognate tyrosine receptor kinase, TrkB. Consistent with this finding, single-cell reverse transcription-polymerase chain reaction experiments showed that one third of the rhythmically active preBötC neurons analysed expressed TrkB mRNA. Moreover, 20% expressed BDNF mRNA, suggesting that the preBötC is both a target and a source of BDNF. At the network level, BDNF augmented activity of preBötC glutamatergic neurons and potentiated glutamatergic synaptic drives in respiratory neurons by 34%. At the cellular level, BDNF increased the activity frequency of endogenously bursting neurons by 53.3% but had no effect on basal membrane properties of respiratory follower neurons, including the Ih current. Our data indicate that BDNF signalling through TrkB can acutely modulate fetal respiratory rhythm in association with increased glutamatergic drive and bursting activity in the preBötC.

Keywords

embryo; endogenous burster neuron; mouse; respiratory neurons; rhythm

Introduction

Neurotrophins regulate nervous system development by controlling the survival and differentiation of specific populations of peripheral and central neurons, particularly in the embryo, fetus and neonate. In addition, some neurotrophins play acute roles in regulating neuronal function throughout life. Brain-derived neurotrophic factor (BDNF) is of particular interest in this regard because it is expressed by many neurons, its synthesis and release are activity dependent (Balkowiec & Katz, 2000, 2002; Lou *et al.*, 2005; Zhou *et al.*, 2006) and it can act on a short time scale to regulate neuronal function (Kovalchuk *et al.*, 2004; Rose *et*

Correspondence: Dr M. Thoby-Brisson, as above. E-mail: muriel.thoby-brisson@inaf.cnrs-gif.fr.
Present address: Institut de Neurobiologie de la Méditerranée, INSERM U29, 13273 Marseille cedex 09, France.

al., 2004; Blum & Konnerth, 2005). For example, BDNF has been shown to regulate neuronal membrane properties and to play important roles in coupling presynaptic neuronal activity to postsynaptic changes in synaptic strength and efficacy (Li *et al.*, 1998; Kafitz *et al.*, 1999; Rose *et al.*, 2004; Blum & Konnerth, 2005; Henneberger *et al.*, 2005). However, relatively little is known about the role of BDNF in the development of complex neural network function.

Previous studies demonstrated that BDNF is required for functional maturation of central respiratory drive (Erickson *et al.*, 1996; Balkowiec & Katz, 1998). One component of the brainstem respiratory network that is known to be a target of BDNF signalling after birth is the preBötzinger complex (preBötC; Thoby-Brisson *et al.*, 2003). The preBötC is required for pacing inspiratory activity (Smith *et al.*, 1991; Feldman & Del Negro, 2006) and is anatomically defined as a group of type 2 vesicular glutamate transporter (VGlut2)-positive interneurons also expressing high levels of neurokinin receptor (NK1R) and somatostatin (Stornetta *et al.*, 2003). Within the preBötC, inspiratory rhythm and pattern generation rely on recurrent glutamate synaptic excitation within the network in combination with activation of intrinsic bursting properties of individual cells (Koshiya & Smith, 1999; Thoby-Brisson *et al.*, 2000; Thoby-Brisson & Ramirez, 2001; Pena *et al.*, 2004). Endogenous bursting neurons, constituting a subset of inspiratory neurons, are capable of generating ectopic bursts of activity between two inspiratory bursts occurring in phase with the population activity (Feldman & Del Negro, 2006) and remain rhythmically active after blockade of excitatory glutamatergic synchronization (Koshiya & Smith, 1999; Thoby-Brisson *et al.*, 2005; Wallen-Mackenzie *et al.*, 2006). Moreover, some respiratory bursting neurons express the Ih current, a conductance known to play an important role in respiratory rhythm modulation (Thoby-Brisson *et al.*, 2000).

Deletion of the BDNF gene leads to disturbances of respiratory rhythmogenesis in newborn mice (Erickson *et al.*, 1996; Balkowiec & Katz, 1998). These findings indicate that BDNF is required before birth for proper development of neuronal circuits controlling breathing, possibly by regulating maturation during fetal development. However, prenatal targets of BDNF signalling in the respiratory network are unknown. The present study was therefore undertaken to test the hypothesis that the preBötC respiratory network is a target of BDNF signalling before birth. In particular, we examined the possibility that BDNF and TrkB play a role in regulating respiratory neuron function during fetal breathing at prenatal day 16.5 in the mouse (Thoby-Brisson *et al.*, 2005), with specific attention towards effects on glutamatergic intra-network communication, endogenous bursting properties and membrane conductances such as the Ih current, all key elements for the respiratory rhythm and pattern generation, some of them being in addition already described as targets for BDNF at postnatal stages (Thoby-Brisson *et al.*, 2003, 2004).

Materials and methods

Experiments were performed in keeping with European and French agricultural ministry guidelines for the care and use of laboratory animals (Council directives 2889 and 86/609/EEC).

In-vitro fetal slice preparation

Brainstem transverse slices were obtained from embryos at embryonic day (E)16.5, E0.5 being the morning after detection of the vaginal plug. Pregnant OF1 mice (Janvier, Le Genest Saint Isle, France) were killed by cervical dislocation and embryos were excised from the uterus and kept at room temperature (24°C) in artificial cerebrospinal fluid bubbled with carbogen (95% O_2/5% CO_2). The artificial cerebrospinal fluid contained (in mM): 120 NaCl, 8 KCl, 1.26 $CaCl_2$, 1.5 $MgCl_2$, 21 $NaHCO_3$, 0.58 Na_2HPO_4, 30 glucose, pH 7.4. Fetal brainstem transverse slices were obtained using the technique previously described by Thoby-Brisson *et al.*

(2005). In brief, the brainstem was isolated from the embryo, embedded in an agar block, mounted onto a vibratome and serially sliced in the transverse plane from rostral to caudal until the posterior limit of the facial nucleus was reached. At 200 μm more caudal from this limit we isolated a 450-μm-thick slice known to contain rhythmically active respiratory neurons of the preBötC at its rostral surface. Slices were then transferred in the recording chamber, continuously perfused with oxygenated artificial cerebrospinal fluid and maintained at 30°C.

Recordings

Population activity recordings were obtained with a glass pipette used as a suction electrode positioned onto the surface of the slice in the preBötC area (see Figs 1A and 3A). The signal was amplified through a high-gain amplifier (7P511; Grass Instruments, Quincy, MA, USA), filtered (low-pass 3 kHz, high-pass 30 Hz), rectified and integrated using an electronic filter (time constant 100 ms; Neurolog system, Digitimer, Hertfordshire, UK), and stored on a computer using the Pclamp9 software (digitizing interface DigiData 1322A; Molecular Devices, Sunnyvale, CA, USA).

Intracellular patch-clamp recordings were obtained from rhythmically active neurons located within 70–100 μm of the macroelectrode in the ventral respiratory group. Patch-clamp recordings were performed under visual control using differential contrast microscopy, an Axoclamp2A amplifier (Molecular Devices) and Pclamp9 software. Patch electrodes were obtained from filamented borosilicate glass tubes (GC 150F; Clark, Pangbourn, UK), filled with a solution containing (in mM): 140 K-gluconic acid, 1 $CaCl_2 \cdot 6H_2O$, 10 EGTA, 2 $MgCl_2 \cdot 6H_2O$, $4Na_2ATP$, 10 HEPES, pH 7.2. When filled with this solution the pipette resistance was 5–6 MΩ. With this solution chloride-mediated synaptic currents appear outward and glutamatergic-mediated synaptic currents appear inward at a holding potential of −50 mV (see Fig. 2B and C). The inhibitory postsynaptic currents (IPSCs) and excitatory postsynaptic currents (EPSCs) can also be distinguished by their decay time (>20 and <2 ms, respectively) and pharmacology; IPSCs are blocked by 10 μM bicuculline and 5 μM strychnine (Wallen-Mackenzie *et al.*, 2006), and EPSCs are blocked by 20 μM 6-cyano-7-nitroquinoxaline-2,3-dione (CNQX) and 50 μM DL-2-amino-5-phosphonovaleric acid (AP5).

Endogenous bursting properties were tested in either current-clamp mode by the capability of the recorded neurons to generate ectopic bursts when compared with population activity in response to depolarizing current injection (Feldman & Del Negro, 2006) or by the persistence of asynchronous rhythmic activity in the presence of 20 μM CNQX alone (Koshiya & Smith, 1999; Thoby-Brisson & Ramirez, 2001) or in a cocktail (see below) containing 20 μM CNQX, 50 μM AP5, 10 μM bicuculline, 5 μM strychnine and 50 μM carbenoxolone (Thoby-Brisson *et al.*, 2000). Even if we did not further examine voltage-dependent pacemaker currents, neurons that fulfilled either of these criteria were categorized as endogenous bursters and the others were considered as follower inspiratory neurons.

Membrane resistance was obtained in voltage-clamp mode. The cells were hyperpolarized with an 80 ms voltage step of −10 mV from a holding voltage of −50 mV. The instantaneous current was measured 30 ms after the onset of the pulse. The Ih current was evoked by applying a series of 2 s hyperpolarizing voltage pulses incrementing in 10 mV from a holding potential of −50 to −110 mV. The Ih current amplitude was measured by subtracting the current amplitude obtained at the end of the voltage step (steady-state current containing the Ih and the instantaneous current) from the current amplitude measured at the beginning of the pulse (containing only the instantaneous current).

Pharmacological agents were dissolved in artificial cerebrospinal fluid and bath applied at final concentrations of: 20 μM for CNQX (Sigma, St Louis, MO, USA), 50 μM for AP5 (Sigma), 5 μM for strychnine (Sigma), 10 μM for bicuculline (Sigma), 50 μM for carbenoxolone (a gap

junction blocker, Sigma), 100 ng/mL for BDNF (Sigma) for 15–30 min, 100 ng/mL for nerve growth factor (Promega, Madison, WI, USA) for 30 min and 200 nM for K252a (Calbiochem, La Jolla, CA, USA) for 1 h. The durations of treatment were chosen in order to allow comparison with previous studies performed at postnatal stages (Thoby-Brisson *et al.*, 2003) and to be compatible with stable patch-clamp recording conditions.

Activity frequency was measured during a 2 min period in the different pharmacological conditions and during 3 min for endogenous burster neurons examined in calcium imaging experiments. Values are given as means ± SEM. Statistical significance was tested using paired difference Student's *t*-test or one-way ANOVA test when appropriate. Values were considered as statistically different when $P < 0.05$.

Calcium imaging

Slices were loaded with the cell-permeant calcium indicator dye Calcium Green 1-AM (10 μm; Molecular Probes) during a 45 min incubation period. The preparation was then placed in the recording chamber where the excess dye was washed out during a 30 min period before image acquisition was performed. Using an E-600-FN upright microscope equipped with a fluorescein filter (Nikon, Tokyo, Japan) and a cooled CCD camera (Coolsnap HQ; Photometrics, Tucson, AZ, USA), fluorescent images were captured in the overlapping mode (simultaneous exposure and readout) with a 100 ms exposure time. Images were analysed using MetaMorph software (Universal Imaging Corporation, West Chester, PA, USA). The changes in fluorescence were normalized to their initial value by expression as the ratio of changes in fluorescence to background fluorescence (ΔF/F).

Single cell multiplex reverse transcription-polymerase chain reaction

Multiplex reverse transcription-polymerase chain reaction (PCR) experiments were performed following the procedure described previously (Cauli *et al.*, 1997; Thoby-Brisson *et al.*, 2003). Whole-cell patch-clamp recordings were obtained from preBötC respiratory neurons defined as being active in phase with the population activity. After 5 min of recording the cytoplasm was aspirated into the recording pipette by application of a gentle negative pressure under visual and electrophysiological controls verifying that the seal was not lost and the holding current remained stable. The content of the pipette were then expelled into a tube containing the elements necessary for reverse transcription and kept at 38°C overnight (Lambolez *et al.*, 1992). We simultaneously detected expression of TrkB, p75, NK1R (substance P receptor neurokinin 1), μ receptor, VGlut2, hyperpolarization-activated cyclic nucleotide-gated non-selective cation channel (HCN)1–4 and BDNF mRNAs. Genomic DNA amplification, which occurred when the nucleus was inadvertently harvested, was assessed for each neuron using a somatostatin gene intron (as a genomic control). After the reverse transcription reaction, the cDNAs were amplified by 20 PCR cycles (30 s at 94°C, 30 s at 60°C and 35 s at 75°C) using 2.5 U of *Taq* polymerase (Qiagen) added with 10 pmol of the primers specified in Table 1. Then, using 2 μL of the first PCR products as a template, 35 cycles of a second PCR were performed with the primers specified in Table 2. PCR fragments of 344, 185, 158, 339, 252, 435, 294, 115, 221 and 151 bp were expected for TrkB, HCN1, HCN2, HCN3, HCN4, VGlut2, NK1R, μ receptor, p75 and BDNF, respectively. A volume of 10 μL of each individual second-step PCR product was then run on a 1.5% agarose gel and stained with ethidium bromide. We used Φx174 cut by *Hae*III with bands at 1353, 1078, 872, 603, 310, 281, 271, 234, 194 and 118 bp, and pBR322 cut by MspI with band at 67, 76, 90, 110, 123, 147, 160, 180, 190, 201, 238–242, 307, 404, 527 and 622 bp as molecular weight markers. As long-lasting patch recordings are incompatible with reverse transcription-PCR analysis, neither endogenous bursting properties nor BDNF effects could be tested for the neurons sampled.

Results

BDNF, but not nerve growth factor, increases the frequency of rhythmic activity in the fetal preBötC network

In 13 slice preparations obtained from E16.5 embryos, exhibiting stable rhythmic activity frequency in control conditions, exogenous application of 100 ng/mL BDNF induced a 43% increase in the frequency of population bursts recorded from the preBötC network after 15 min and a 51% increase after 30 min (Fig. 1A–D). Mean frequency values changed from 11.1 ± 0.8 bursts/min in control conditions to 15.9 ± 0.6 bursts/min after 15 min of BDNF treatment and to 16.8 ± 0.7 bursts/min after 30 min (*t*-test, $P < 0.0005$; Fig. 1E). Values obtained after 15 and 30 min were not statistically different (*t*-test, $P = 0.35$), suggesting that application of BDNF reached its maximum effect within 15 min (see Fig. 1D), a delay compatible with a non-genomic effect of the neurotrophin on neuronal excitability.

In six additional preparations, a 30 min application of 100 ng/mL nerve growth factor, another neurotrophin sharing a high degree of sequence homology with BDNF but acting through a distinct signalling pathway via activation of a different tyrosine kinase receptor type (TrkA; Ultsch *et al.*, 1999; Patapoutian & Reichardt, 2001), had no significant effect on the rhythmic activity frequency (11 ± 0.8 bursts/min in control conditions vs. 12.5 ± 0.8 bursts/min in the presence of nerve growth factor; *t*-test, $P = 0.72$; Fig. 1E). These experiments show that the respiratory network activity can be specifically modulated by BDNF at prenatal stages, with a delay of action similar to that known for classical neuromodulators in the same preparation.

BDNF increases glutamatergic synaptic inputs in the fetal preBötC network

As respiratory pattern and rhythm generation in the preBötC network relies in part on glutamatergic synaptic connections, we aimed at examining the effect of BDNF on excitatory glutamatergic neurotransmission in rhythmically active neurons within the fetal preBötC (Fig. 2A). Voltage-clamp recordings revealed that fetal inspiratory neurons receive both chloride-mediated synaptic currents (blocked by 10 μM bicuculline and 5 μM strychnine) and glutamate-mediated synaptic currents (blocked by 20 μM CNQX, Fig. 2C) in between two inspiratory bursts (Fig. 2B, ellipse and Fig. 2C), whereas the synaptic drive underlying inspiratory bursts is glutamate mediated (Fig. 2D). We performed synaptic current analysis on seven preBötC neurons exhibiting no evidence of endogenous bursting properties from seven slice preparations, for which we analysed an average of 150 glutamatergic events and 150 chloride-mediated events in periods between inspiratory bursts. First, we characterized the effect of the neurotrophin on glutamatergic currents spontaneously generated between individual rhythmic inspiratory bursts. The amplitude (27 ± 5 pA in control vs. 23 ± 6 pA in BDNF for 15 min; *t*-test, $P = 0.25$) and decay time (1.77 ± 0.2 ms in control vs. 1.91 ± 0.2 ms in BDNF for 15 min; *t*-test, $P = 0.29$) of the EPSC were unaffected by BDNF application. In contrast, BDNF exposure induced a significant increase in the frequency of spontaneous EPSCs (compare Fig. 2E with F). The mean frequency augmented from 9.75 ± 0.7 events/s in control to 13.9 ± 0.9 events/s in the presence of BDNF (*t*-test, $P < 0.0005$; Fig. 2G). Second, we analysed the effect of BDNF on chloride-mediated currents between inspiratory bursts. The amplitude (10.06 ± 2.7 pA in control vs. 8.21 ± 0.86 pA in BDNF for 15 min; *t*-test, $P = 0.5$), decay time (23.02 ± 3.4 ms in control vs. 27.27 ± 3.01 ms in BDNF for 15 min; *t*-test, $P = 0.4$) and frequency (6.61 ± 0.75 events/s in control vs. 8 ± 0.88 events/s in the presence of BDNF; *t*-test, $P > 0.05$; Fig. 2E–G) of IPSCs were not significantly affected by BDNF application. Thus, BDNF increases the activity of glutamatergic neurons without affecting chloride-mediated synaptic events.

Synchronization within the preBötC results from the summation of glutamatergic EPSCs forming the depolarizing drive underlying respiratory-related bursts (Fig. 2B, rectangle and

Fig. 2D). We therefore examined whether the excitatory effect of BDNF on glutamatergic events resulted in changes of the respiratory drive. The amplitude of the inward synaptic drive was measured in control conditions and after 15 min exposure to BDNF in eight neurons held at −50 mV (Fig. 2H and I). The mean amplitude values obtained from 10 consecutive bursts increased significantly (t-test, $P = 0.006$) from 14.7 ± 1.2 pA in control to 19.7 ± 1.3 pA after treatment (Fig. 2I and J). As a consequence, the number of action potentials (APs) generated during the burst was increased from 4.1 ± 0.3 APs/burst in control to 5.6 ± 0.4 APs/burst in the presence of BDNF (*t*-test, $P = 0.009$). Overall, these experiments revealed an excitatory action of BDNF on the activity of the glutamatergic neuronal population controlling the synchronization within the fetal preBötC network.

BDNF modulates the activity of endogenous bursting neurons in the fetal preBötC

We next investigated whether BDNF had a specific effect on the activity of respiratory neurons exhibiting endogenous bursting properties. In order to increase the probability of recording this type of cell, which represents a small proportion of preBötC neurons overall (Pena *et al.*, 2004), we used calcium imaging, which allows us to visualize calcium changes that reflect electrical activity (Thoby-Brisson *et al.*, 2005) simultaneously in a large number of cells in a single preparation (41 ± 5 rhythmic cells/slice, range 23–78 cells/slice, $n = 15$). In control conditions individual cells showed spontaneous changes in fluorescence (traces 1–10 in Fig. 3A) occurring in phase with changes observed in the preBötC area as a whole (green trace in Fig. 3A) and in phase with electrical activity recorded in the preBötC region (integrated trace in Fig. 3A).

Blockade of connectivity in slice preparations with the application of 20 μM CNQX ($n = 8$) or a cocktail containing 20 μM CNQX, 50 μM AP5, 10 μM bicuculline, 5 μM strychnine and 50 μM carbenoxolone ($n = 7$) suppressed synchronized calcium events. This results in the absence of rhythmically organized calcium changes in the preBötC area (see the green and integrated traces in Fig. 3B). In these conditions, only a few cells continued to exhibit rhythmic calcium variations (cells 1 and 6 in Fig. 3B), a property assigned to endogenous bursters (Koshiya & Smith, 1999). Among 620 cells analysed from 15 preparations we found 47 bursting neurons (7.6% of the total population analysed), with 20 bursting neurons identified in the presence of CNQX and 27 bursting neurons identified in the presence of the cocktail.

Exogenous application of BDNF had a significant effect on calcium transients in these cells. Indeed, the presence of the neurotrophin induced a 53.3% increase in the frequency of rhythmically organized calcium variations in 40 of 47 isolated bursting neurons (see traces 1 and 6, Fig. 3C). The mean frequency of rhythmic calcium changes augmented from 3.1 ± 0.5 calcium transients/min in CNQX to 4.3 ± 0.6 calcium transients/min in the presence of BDNF (*t*-test, $P = 0.0004$) and from 3.01 ± 0.2 calcium transients/min in cocktail to 4.6 ± 0.3 calcium transients/min in the presence of BDNF (*t*-test, $P = 0.0002$). In contrast, for the seven remaining endogenous bursters, application of BDNF induced no significant changes in the frequency of calcium changes (3.4 ± 1.04 transients/min in cocktail and 3.1 ± 0.9 calcium transients/min in the presence of BDNF; t-test, $P = 0.82$). These data indicate that BDNF increases the activity of most of the respiratory bursting neurons by increasing the frequency of rhythmically organized calcium changes, thereby probably enhancing their ability to produce bursts. Altogether, we conclude that the excitatory effects of BDNF on the fetal preBötC network include an increase of activity in 85% of endogenous bursters.

Basal membrane properties of fetal follower rhythmic neurons are not affected by BDNF

The BDNF-induced increases observed in the frequency of bursting neuron activity, the activity of glutamatergic neurons and the respiratory frequency could possibly be explained by changes in the membrane properties of rhythmically active neurons. The frequency increase could

simply result from a depolarization of the membrane potential of respiratory neurons. However, whole-cell patch-clamp recordings performed on eight rhythmically active neurons exhibiting no evidence of endogenous bursting properties revealed that the mean resting membrane potential value was unaffected by BDNF (mean values −52.7 ± 1.3 mV in control vs. −51.1 ± 1.8 mV in BDNF, *t*-test, $P = 0.49$; Fig. 4A and B). Similarly, membrane resistance and burst duration remained unchanged after 15 min exposure to BDNF (*t*-test, $P = 0.38$). The mean values were 1547 ± 312 MΩ in control vs. 1213 ± 197 MΩ in BDNF and 616 ± 36 ms in control vs. 606 ± 29 ms in BDNF for membrane resistance and burst duration, respectively (Fig. 4B).

We also examined the Ih current because (i) this conductance is known to play an important role in respiratory rhythm modulation (Thoby-Brisson *et al.*, 2000), (ii) the Ih current is expressed by some respiratory neurons exhibiting pacemaker properties (Thoby-Brisson *et al.*, 2000; Thoby-Brisson & Ramirez, 2001) and (iii) the Ih current is known to be a target for BDNF at postnatal stages (Thoby-Brisson *et al.*, 2003). In seven rhythmic neurons expressing the Ih current, BDNF exposure induced no significant changes in its amplitude over a voltage range from −50 to −110 mV. One example is illustrated in Fig. $4C_1$ (control) and Fig. $4C_2$ (after BDNF treatment). The mean current amplitude obtained for a voltage step from −50 to −110 mV remained similar in control conditions (49 ± 13 pA) and in the presence of BDNF (46 ± 13 pA; *t*-test, $P = 0.86$; Fig. 4D). Thus, the membrane properties of the follower neurons that we tested, which may be involved in the modulation of respiratory rhythm, appear not to be affected by exogenous BDNF.

BDNF acts through activation of TrkB receptors expressed by fetal preBötC neurons

To begin to define the signalling pathway through which BDNF acts on fetal respiratory neurons we tested the requirement for activation of the tyrosine kinase receptor TrkB, a high-affinity binding site for BDNF. In a first set of experiments embryonic slices were pretreated with the tyrosine kinase inhibitor K252a (200 nM) for 1 h. The frequency of the preBötC rhythmic activity was similar (ANOVA) in control conditions (12.4 ± 1.1 bursts/min), in the presence of K252a (12 ± 1 bursts/min; $P = 0.8$) and in the presence of K252a plus BDNF (11.5 ± 0.7 bursts/min; $P = 0.91$; $n = 5$; Fig. 5A). Thus, the effects of BDNF on respiratory frequency were abolished in the presence of K252a, suggesting that TrkB activation is required to mediate the effect of BDNF on respiratory frequency.

In a second set of experiments, the expression of mRNAs encoding proteins involved in BDNF signalling was examined in functionally identified respiratory neurons using single-cell multiplex reverse transcription-PCR. In 22 rhythmically active preBötC neurons (without distinction between endogenous bursters or follower neurons) we examined the expression of mRNAs encoding TrkB, the pan-neurotrophin receptor p75 and the hyperpolarization-activated non-selective cationic channel subunits of the Ih current (HCN1-4), as well as mRNAs encoding possible markers of inspiratory neurons, such as the NK1R, the μ opioid receptor and for the vesicular transporter VGlut2. It is very likely that these mRNAs give rise to functional proteins as (i) the Ih and glutamatergic currents are detectable in the fetal neurons recorded, (ii) BDNF modulates preBötC network activity and has direct effects on the bursting frequency of some respiratory neurons and (iii) the modulation by substance P and opioid agonists is already effective at the examined stage (Thoby-Brisson *et al.*, 2005). Of the 22 cells tested, seven (32%) expressed TrkB mRNA and all of these co-expressed at least one of the HCN subunit mRNAs (Fig. 5B and C); three-seventh of the TrkB-expressing neurons also expressed VGlut2 mRNA, two-seventh co-expressed the μ receptor mRNA and only one neuron co-expressed NK1R (Fig. 5C), proportions that are similar to those described in the newborn (Thoby-Brisson *et al.*, 2003). p75 mRNA was found in five neurons (23%), two of which also expressed TrkB mRNA (Fig. 5B and C). The fact that a significant subset of rhythmically active neurons expresses TrkB mRNA is consistent with fetal preBötC neurons

being a direct target of BDNF. Moreover, the mRNA encoding BDNF itself was found in two out of 10 neurons tested, suggesting that some preBötC neurons could themselves be a source of BDNF within the fetal respiratory network.

Discussion

The present study demonstrates that BDNF can acutely regulate respiratory rhythmogenesis in the fetal mouse brainstem slice preparation. In particular, exogenous BDNF increases respiratory frequency in the preBötC, a key site for respiratory pattern generation, through a potentiation of excitatory glutamatergic synaptic drives associated with a frequency increase in the activity of endogenously bursting neurons; 32% of rhythmically active neurons tested express mRNA encoding the TrkB receptor, consistent with a direct action of BDNF on a subset of preBötC neurons. Thus, in addition to long-term effects on the survival and maturation of respiratory-related neurons (Katz, 2005), BDNF signalling may also be important for acute modulation of the fetal respiratory rhythmogenic network.

Fetal respiratory rhythm regulation by BDNF is associated with modifications in glutamatergic signalling and activity of endogenous bursting neurons in the preBötC

From *in-vitro* experiments performed on preparations obtained at postnatal stages it is considered that respiratory rhythm and pattern generation rely on interplay between glutamatergic connections and bursting properties expressed in a subset of respiratory neurons (Rekling & Feldman, 1998; Del Negro *et al.*, 2002; Pena *et al.*, 2004; Feldman & Del Negro, 2006). The present data show that, in the embryo, BDNF modulates the activity of the preBötC by enhancing the excitatory glutamatergic synaptic drive underlying bursting discharge and the intrinsic bursting frequency of isolated endogenous bursting neurons. It is possible that increased activity of endogenous bursters may contribute to the increase in respiratory frequency of the whole network. However, the discrepancy between the proportion of TrkB-positive neurons in the preBötC on the one hand (32%) and the number of rhythmic neurons exhibiting endogenous bursting properties on the other (<10%) indicates that bursting neurons are not the only target for BDNF within the respiratory neural network. In addition, potentiation of glutamatergic synaptic drive could result from either the increase in the discharge during bursts of activity in presynaptic glutamatergic neurons, some of which are endogenous bursters, a direct effect of BDNF on glutamatergic transmission (for review see Lessmann, 1998) or both. At the same time, increased synaptic drive could augment the intra-burst discharge in postsynaptic neurons including in bursting neurons. Thus, these two effects of BDNF, on activity of endogenous bursting neurons and glutamatergic synaptic drive, respectively, could work in concert to increase the activity of the network as a whole. It has to be emphasized that the implication of endogenous bursting neurons in respiratory rhythmogenesis and functional breathing activity is still controversial at postnatal (Roland *et al.*, 1980; Paton & St-John, 2007; Ramirez & Garcia, 2007) as well as at prenatal stages. BDNF-induced modulation mechanisms are certainly more complex when considering the fully intact fetal respiratory system.

We observed BDNF effects on endogenous bursting neuron activity after isolation of these cells from their synaptic partners in the respiratory network. This suggests that BDNF alters bursting activity by acting directly on membrane properties such as voltage-dependent conductances. One possibility is that BDNF accelerates the bursting frequency of these cells by bringing the membrane potential to values compatible with a stronger activation of pacemaker currents. Moreover, given that bursting neurons within the respiratory neural network are heterogeneous and that their activity relies on sodium-dependent conductances, calcium currents and/or the Ih current (Thoby-Brisson *et al.*, 2000; Thoby-Brisson & Ramirez, 2001; Pena *et al.*, 2004), it is possible that BDNF differentially modulates the activity of distinct

pacemaker subtypes. However, analyses of BDNF effects on bursting neuron membrane properties within the preBötC will be required to address these possibilities.

BDNF modulation of respiratory rhythm is distinct in fetal and newborn mice

We previously identified a neuromodulatory action of BDNF on properties of the respiratory network in newborn animals. In contrast to the current findings in the fetus, exposure of the newborn mouse brainstem slice to BDNF results in a decrease in respiratory frequency (Thoby-Brisson *et al.*, 2003). This decrease is associated with increased glutamatergic drives and a significant reduction in the Ih current amplitude. First, the fact that at both developmental stages examined (pre- and postnatal) we found an increase in the glutamatergic synaptic drive but opposite effects on the frequency suggests that these two parameters are not directly linked. Second, at prenatal stages, the Ih current is unaffected by BDNF and is smaller in amplitude than after birth (Thoby-Brisson *et al.*, 2000). Thus, there is a developmental switch in the effect of BDNF on respiratory frequency between E16.5 and postnatal days 1–4 that may rely in part on the maturation of membrane properties in preBötC neurons, including the Ih current. This possibility is consistent with findings in other neuronal populations that maturation of the Ih current can contribute to the shaping of rhythmic activity (Di Pasquale *et al.*, 1996; Vasilyev & Barish, 2002). More generally, development of the Ih current is hypothesized to strongly contribute to functional maturation of neuronal circuits (Rocha *et al.*, 2006). Interestingly, we found that all fetal rhythmic neurons expressing the TrkB receptor mRNA also expressed HCN mRNAs at E16.5, despite the fact that TrkB signalling and Ih current modulation are not yet linked at this stage. We hypothesize, therefore, that the functional maturation of pathways linking TrkB receptor activation and Ih may be a critical step in the development of BDNF modulation of respiratory rhythmogenesis in the preBötC. Further experiments are required to test this hypothesis and should also be extended to other conductances known to play important roles in respiratory rhythmogenesis, such as persistant sodium current and calcium-activated non-specific cationic current (Thoby-Brisson & Ramirez, 2001; Del Negro *et al.*, 2002, 2005; Pena *et al.*, 2004; Paton *et al.*, 2006).

Age-dependent effects of BDNF-induced acute modulation have also been observed after birth in other parts of the central nervous system. For example, in the spinal cord, BDNF-induced depression of EPSCs in motoneurons was observed only during the first postnatal week (Arvanian & Mendell, 2001). In the Kölliker–Fuse nucleus, another structure related to respiration, the strength and direction of BDNF-mediated modulation of glutamatergic synaptic activity depend on the developmental stage (Kron *et al.*, 2007a) and the depressant effect of BDNF on spontaneous IPSC amplitude was significant only during the first 10 days after birth (Kron *et al.*, 2007b). In the context of the preBötC, changes in the effect of BDNF on respiratory rhythm generated in the preBötC probably occur around birth. This earlier switch is possibly due to the fact that the Kölliker-Fuse nucleus and preBötC exhibit completely different maturational profiles and, most probably, the preBötC is more mature at birth than the Kölliker–Fuse nucleus (Dutschmann *et al.*, 2004).

Acute and trophic actions of BDNF

Deletion of the gene encoding BDNF results in severe respiratory disturbances, including depressed and irregular ventilation associated with dysfunction of the central respiratory generator and loss of peripheral chemoreceptor inputs (Erickson *et al.*, 1996; Balkowiec & Katz, 1998). These defects are due in part to developmental deficits linked to the lack of neurotrophic action of BDNF during embryonic development (Erickson *et al.*, 1996; Balkowiec & Katz, 1998). Because a rhythm is still generated in the reduced brainstem preparation obtained from $BDNF^{-/-}$ animals it is tempting to consider that BDNF is not necessary for establishment of the rhythm generator but rather for maturation of the central respiratory controller and some of the properties of its constitutive elements (Balkowiec & Katz, 1998).

Given that neural activity is itself a critical developmental cue required for normal maturation of embryonic motor circuits (Hanson & Landmesser, 2004), the present data suggest that respiratory abnormalities observed in newborn animals that are deficient in BDNF might reflect a lack of acute neuromodulatory action in the fetal respiratory network as well as neurotrophic defects. This possibility is consistent with observations that BDNF plays a critical role in activity-dependent maturation of synaptic connections (Shen *et al.*, 2006). Moreover, given the fact that (i) the preBötC itself contains neurons expressing mRNA coding for BDNF, (ii) BDNF increases activity in the preBötC network and (iii) the release of the neurotrophin is activity-dependent, it is possible that the maturation and modulation of respiratory network activity are reciprocally related by an autocrine/paracrine action of BDNF within the respiratory network.

More generally, our findings may be relevant to understanding the pathophysiology of respiratory dysfunction in Rett syndrome, a severe progressive neurological disorder caused by loss of function mutations in the gene encoding the transcription factor methyl-CpG binding protein 2 (MeCP2) (Van den Veyver & Zoghbi, 2000; Bienvenu & Chelly, 2006; Francke, 2006). Indeed, MeCP2 is known to regulate BDNF transcription (Chen *et al.*, 2003; Wade, 2004; Chang *et al.*, 2006; Zhou *et al.*, 2006) and mouse models in which MeCP2 is deleted exhibit severely depressed levels of BDNF in the brainstem (Wang *et al.*, 2006; Ogier *et al.*, 2007), abnormal BDNF secretion (Wang *et al.*, 2006; Ogier *et al.*, 2007) and respiratory breathing phenotypes (Viemari *et al.*, 2005; Ogier *et al.*, 2007) similar to respiratory dysfunction in Rett syndrome (Elian & Rudolf, 1991; Kerr, 1992; Kerr & Julu, 1999; Julu *et al.*, 2001; Weese-Mayer *et al.*, 2006). Although the respiratory phenotype in Rett syndrome appears late in postnatal development (i.e. a few months after birth in mice and 1.5–2 years in human), there is increasing evidence for early neuronal defects (Einspieler *et al.*, 2005; Medrihan *et al.*, 2008). For example, MeCP2-deficient neurons already exhibit abnormal BDNF secretion at birth (Wang *et al.*, 2006; Ogier *et al.*, 2007). It will therefore be important to determine whether or not prenatal disruption of BDNF signalling in the preBötC is a consequence of MeCP2 deficiency that contributes to respiratory network dysfunction in Rett syndrome.

Acknowledgements

This work was supported by the Centre National de la Recherche Scientifique for NGI, Institut National de la Santé et de la Recherche Médicale (M.T.-B.) and the U.S. National Heart, Lung and Blood Institute (D.M.K.).

Abbreviations

AP
: action potential

AP5
: DL-2-amino-5-phosphonovaleric acid

BDNF
: brain-derived neurotrophic factor

CNQX
: 6-cyano-7-nitroquinoxaline-2,3-dione

E
: embryonic day

EPSC
: excitatory postsynaptic current

HCN
hyperpolarization-activated cyclic nucleotide-gated non-selective channel

IPSC
inhibitory postsynaptic current

MeCP2
methyl-CpG binding protein 2

PCR
polymerase chain reaction

preBötC
preBötzinger complex

VGlut2
type 2 vesicular glutamate transporter

References

Arvanian VL, Mendell LM. Acute modulation of synaptic transmission to motoneurons by BDNF in the neonatal rat spinal cord. Eur J Neurosci 2001;14:1800–1808. [PubMed: 11860475]

Balkowiec A, Katz DM. Brain-derived neurotrophic factor is required for normal development of the central respiratory rhythm in mice. J Physiol 1998;510(Pt 2):527–533. [PubMed: 9706001]

Balkowiec A, Katz DM. Activity-dependent release of endogenous brain-derived neurotrophic factor from primary sensory neurons detected by ELISA in situ. J Neurosci 2000;20:7417–7423. [PubMed: 11007900]

Balkowiec A, Katz DM. Cellular mechanisms regulating activity-dependent release of native brain-derived neurotrophic factor from hippocampal neurons. J Neurosci 2002;22:10399–10407. [PubMed: 12451139]

Bienvenu T, Chelly J. Molecular genetics of Rett syndrome: when DNA methylation goes unrecognized. Nat Rev 2006;7:415–426.

Blum R, Konnerth A. Neurotrophin-mediated rapid signaling in the central nervous system: mechanisms and functions. Physiology (Bethesda) 2005;20:70–78. [PubMed: 15653842]

Cauli B, Audinat E, Lambolez B, Angulo MC, Ropert N, Tsuzuki K, Hestrin S, Rossier J. Molecular and physiological diversity of cortical nonpyramidal cells. J Neurosci 1997;17:3894–3906. [PubMed: 9133407]

Chang Q, Khare G, Dani V, Nelson S, Jaenisch R. The disease progression of Mecp2 mutant mice is affected by the level of BDNF expression. Neuron 2006;49:341–348. [PubMed: 16446138]

Chen WG, Chang Q, Lin Y, Meissner A, West AE, Griffith EC, Jaenisch R, Greenberg ME. Derepression of BDNF transcription involves calcium-dependent phosphorylation of MeCP2. Science 2003;302:885–889. [PubMed: 14593183]

Del Negro CA, Morgado-Valle C, Feldman JL. Respiratory rhythm: an emergent network property? Neuron 2002;34:821–830. [PubMed: 12062027]

Del Negro CA, Morgado-Valle C, Hayes JA, Mackay DD, Pace RW, Crowder EA, Feldman JL. Sodium and calcium current-mediated pacemaker neurons and respiratory rhythm generation. J Neurosci 2005;25:446–453. [PubMed: 15647488]

Di Pasquale E, Tell F, Monteau R, Hilaire G. Perinatal developmental changes in respiratory activity of medullary and spinal neurons: an in vitro study on fetal and newborn rats. Brain Res 1996;91:121–130.

Dutschmann M, Morschel M, Kron M, Herbert H. Development of adaptive behaviour of the respiratory network: implications for the pontine Kolliker–Fuse nucleus. Respir Physiol Neurobiol 2004;143:155–165. [PubMed: 15519552]

Einspieler C, Kerr AM, Prechtl HF. Is the early development of girls with Rett disorder really normal? Pediatr Res 2005;57:696–700. [PubMed: 15718369]

Elian M, Rudolf ND. EEG and respiration in Rett syndrome. Acta Neurol Scand 1991;83:123–128. [PubMed: 2017897]

Erickson JT, Conover JC, Borday V, Champagnat J, Barbacid M, Yancopoulos G, Katz DM. Mice lacking brain-derived neurotrophic factor exhibit visceral sensory neuron losses distinct from mice lacking NT4 and display a severe developmental deficit in control of breathing. J Neurosci 1996;16:5361–5371. [PubMed: 8757249]

Feldman JL, Del Negro CA. Looking for inspiration: new perspectives on respiratory rhythm. Nat Rev 2006;7:232–242.

Francke U. Mechanisms of disease: neurogenetics of MeCP2 deficiency. Nat Clin Pract 2006;2:212–221.

Hanson MG, Landmesser LT. Normal patterns of spontaneous activity are required for correct motor axon guidance and the expression of specific guidance molecules. Neuron 2004;43:687–701. [PubMed: 15339650]

Henneberger C, Juttner R, Schmidt SA, Walter J, Meier JC, Rothe T, Grantyn R. GluR- and TrkB-mediated maturation of GABA receptor function during the period of eye opening. Eur J Neurosci 2005;21:431–440. [PubMed: 15673442]

Julu PO, Kerr AM, Apartopoulos F, Al-Rawas S, Engerstrom IW, Engerstrom L, Jamal GA, Hansen S. Characterisation of breathing and associated central autonomic dysfunction in the Rett disorder. Arch Dis Child 2001;85:29–37. [PubMed: 11420195]

Kafitz KW, Rose CR, Thoenen H, Konnerth A. Neurotrophin-evoked rapid excitation through TrkB receptors. Nature 1999;401:918–921. [PubMed: 10553907]

Katz DM. Regulation of respiratory neuron development by neurotrophic and transcriptional signaling mechanisms. Respir Physiol Neurobiol 2005;149:99–109. [PubMed: 16203214]

Kerr AM. A review of the respiratory disorder in the Rett syndrome. Brain Dev 1992;14(Suppl):S43–S45. [PubMed: 1626633]

Kerr AM, Julu PO. Recent insights into hyperventilation from the study of Rett syndrome. Arch Dis Child 1999;80:384–387. [PubMed: 10086952]

Koshiya N, Smith JC. Neuronal pacemaker for breathing visualized in vitro. Nature 1999;400:360–363. [PubMed: 10432113]

Kovalchuk Y, Holthoff K, Konnerth A. Neurotrophin action on a rapid timescale. Curr Opin Neurobiol 2004;14:558–563. [PubMed: 15464888]

Kron M, Morschel M, Reuter J, Zhang W, Dutschmann M. Developmental changes in brain-derived neurotrophic factor-mediated modulations of synaptic activities in the pontine Kolliker–Fuse nucleus of the rat. J Physiol 2007a;583:315–327. [PubMed: 17569735]

Kron M, Zhang W, Dutschmann M. Developmental changes in the BDNF-induced modulation of inhibitory synaptic transmission in the Kolliker–Fuse nucleus of rat. Eur J Neurosci 2007b;26:3449–3457. [PubMed: 18052976]

Lambolez B, Audinat E, Bochet P, Crepel F, Rossier J. AMPA receptor subunits expressed by single Purkinje cells. Neuron 1992;9:247–258. [PubMed: 1323310]

Lessmann V. Neurotrophin-dependent modulation of glutamatergic synaptic transmission in the mammalian CNS. Gen Pharmacol 1998;31:667–674. [PubMed: 9809461]

Li YX, Zhang Y, Lester HA, Schuman EM, Davidson N. Enhancement of neurotransmitter release induced by brain-derived neurotrophic factor in cultured hippocampal neurons. J Neurosci 1998;18:10231–10240. [PubMed: 9852560]

Lou H, Kim SK, Zaitsev E, Snell CR, Lu B, Loh YP. Sorting and activity-dependent secretion of BDNF require interaction of a specific motif with the sorting receptor carboxypeptidase e. Neuron 2005;45:245–255. [PubMed: 15664176]

Medrihan L, Tantalaki E, Aramuni G, Sargsyan V, Dudanova I, Missler M, Zhang W. Early defects of GABAergic synapses in the brain stem of a MeCP2 mouse model of rett syndrome. J Neurophysiol 2008;99:112–121. [PubMed: 18032561]

Ogier M, Wang H, Hong E, Wang Q, Greenberg ME, Katz DM. Brain-derived neurotrophic factor expression and respiratory function improve after ampakine treatment in a mouse model of Rett syndrome. J Neurosci 2007;27:10912–10917. [PubMed: 17913925]

Patapoutian A, Reichardt LF. Trk receptors: mediators of neurotrophin action. Curr Opin Neurobiol 2001;11:272–280. [PubMed: 11399424]

Paton JF, St-John WM. Counterpoint: medullary pacemaker neurons are essential for gasping, but not eupnea, in mammals. J Appl Physiol 2007;103:718–720. [PubMed: 17666729]

Paton JF, Abdala AP, Koizumi H, Smith JC, St-John WM. Respiratory rhythm generation during gasping depends on persistent sodium current. Nat Neurosci 2006;9:311–313. [PubMed: 16474390]

Pena F, Parkis MA, Tryba AK, Ramirez JM. Differential contribution of pacemaker properties to the generation of respiratory rhythms during normoxia and hypoxia. Neuron 2004;43:105–117. [PubMed: 15233921]

Ramirez JM, Garcia A III. Point: medullary pacemaker neurons are essential for both eupnea and gasping in mammals. J Appl Physiol 2007;103:717–718. [PubMed: 17272416]Discussion 722

Rekling JC, Feldman JL. PreBotzinger complex and pacemaker neurons: hypothesized site and kernel for respiratory rhythm generation. Annu Rev Physiol 1998;60:385–405. [PubMed: 9558470]

Rocha N, Rolfs A, Strauss U. Ih is maturing: implications for neuronal development. Neurodegener Dis 2006;3:27–31. [PubMed: 16909033]

Roland PE, Larsen B, Lassen NA, Skinhoj E. Supplementary motor area and other cortical areas in organization of voluntary movements in man. J Neurophysiol 1980;43:118–136. [PubMed: 7351547]

Rose CR, Blum R, Kafitz KW, Kovalchuk Y, Konnerth A. From modulator to mediator: rapid effects of BDNF on ion channels. Bioessays 2004;26:1185–1194. [PubMed: 15499580]

Shen W, Wu B, Zhang Z, Dou Y, Rao ZR, Chen YR, Duan S. Activity-induced rapid synaptic maturation mediated by presynaptic cdc42 signaling. Neuron 2006;50:401–414. [PubMed: 16675395]

Smith JC, Ellenberger HH, Ballanyi K, Richter DW, Feldman JL. Pre-Botzinger complex: a brainstem region that may generate respiratory rhythm in mammals. Science 1991;254:726–729. [PubMed: 1683005]

Stornetta RL, Rosin DL, Wang H, Sevigny CP, Weston MC, Guyenet PG. A group of glutamatergic interneurons expressing high levels of both neurokinin-1 receptors and somatostatin identifies the region of the pre-Botzinger complex. J Comp Neurol 2003;455:499–512. [PubMed: 12508323]

Thoby-Brisson M, Ramirez JM. Identification of two types of inspiratory pacemaker neurons in the isolated respiratory neural network of mice. J Neurophysiol 2001;86:104–112. [PubMed: 11431492]

Thoby-Brisson M, Telgkamp P, Ramirez JM. The role of the hyperpolarization-activated current in modulating rhythmic activity in the isolated respiratory network of mice. J Neurosci 2000;20:2994–3005. [PubMed: 10751452]

Thoby-Brisson M, Cauli B, Champagnat J, Fortin G, Katz DM. Expression of functional tyrosine kinase B receptors by rhythmically active respiratory neurons in the pre-Botzinger complex of neonatal mice. J Neurosci 2003;23:7685–7689. [PubMed: 12930808]

Thoby-Brisson M, Autran S, Fortin G, Champagnat J. BDNF preferentially targets membrane properties of rhythmically active neurons in the pre-Botzinger complex in neonatal mice. Adv Exp Med Biol 2004;551:115–120. [PubMed: 15602952]

Thoby-Brisson M, Trinh JB, Champagnat J, Fortin G. Emergence of the pre-Botzinger respiratory rhythm generator in the mouse embryo. J Neurosci 2005;25:4307–4318. [PubMed: 15858057]

Ultsch MH, Wiesmann C, Simmons LC, Henrich J, Yang M, Reilly D, Bass SH, de Vos AM. Crystal structures of the neurotrophin-binding domain of TrkA, TrkB and TrkC. J Mol Biol 1999;290:149–159. [PubMed: 10388563]

Van den Veyver IB, Zoghbi HY. Methyl-CpG-binding protein 2 mutations in Rett syndrome. Curr Opin Genet Dev 2000;10:275–279. [PubMed: 10826991]

Vasilyev DV, Barish ME. Postnatal development of the hyperpolarization-activated excitatory current Ih in mouse hippocampal pyramidal neurons. J Neurosci 2002;22:8992–9004. [PubMed: 12388606]

Viemari JC, Maussion G, Bevengut M, Burnet H, Pequignot JM, Nepote V, Pachnis V, Simonneau M, Hilaire G. Ret deficiency in mice impairs the development of A5 and A6 neurons and the functional maturation of the respiratory rhythm. Eur J Neurosci 2005;22:2403–2412. [PubMed: 16307583]

Wade PA. Dynamic regulation of DNA methylation coupled transcriptional repression: BDNF regulation by MeCP2. Bioessays 2004;26:217–220. [PubMed: 14988922]

Wallen-Mackenzie A, Gezelius H, Thoby-Brisson M, Nygard A, Enjin A, Fujiyama F, Fortin G, Kullander K. Vesicular glutamate transporter 2 is required for central respiratory rhythm generation but not for locomotor central pattern generation. J Neurosci 2006;26:12294–12307. [PubMed: 17122055]

Wang H, Chan SA, Ogier M, Hellard D, Wang Q, Smith C, Katz DM. Dysregulation of brain-derived neurotrophic factor expression and neurosecretory function in Mecp2 null mice. J Neurosci 2006;26:10911–10915. [PubMed: 17050729]

Weese-Mayer DE, Lieske SP, Boothby CM, Kenny AS, Bennett HL, Silvestri JM, Ramirez JM. Autonomic nervous system dysregulation: breathing and heart rate perturbation during wakefulness in young girls with Rett syndrome. Pediatr Res 2006;60:443–449. [PubMed: 16940240]

Zhou Z, Hong EJ, Cohen S, Zhao WN, Ho HY, Schmidt L, Chen WG, Lin Y, Savner E, Griffith EC, Hu L, Steen JA, Weitz CJ, Greenberg ME. Brain-specific phosphorylation of MeCP2 regulates activity-dependent Bdnf transcription, dendritic growth, and spine maturation. Neuron 2006;52:255–269. [PubMed: 17046689]

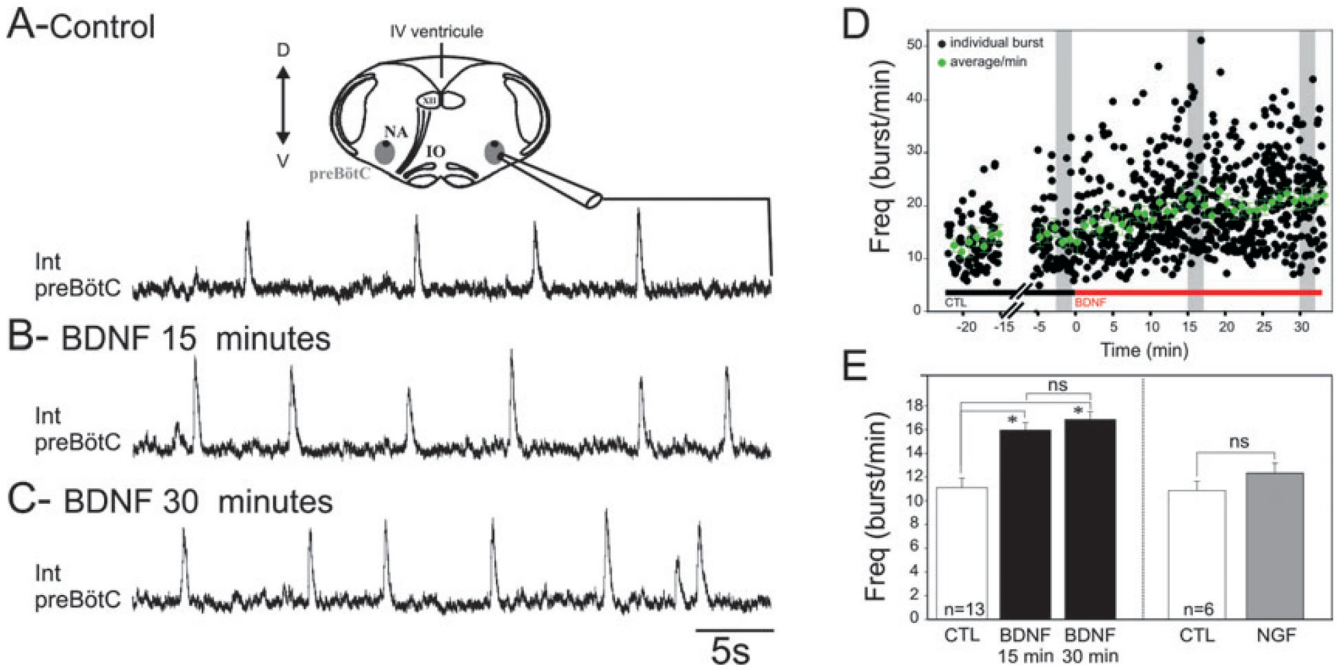

Fig. 1.

BDNF increases respiratory frequency in the fetal mouse transverse brainstem slice preparation. Integrated population activity recorded from the preBötC respiratory network in control conditions (A) and after 15 min (B) and 30 min (C) exposure to 100 ng/mL BDNF. (A) Top: Schematic diagram of a transverse brainstem slice containing the preBötC from which population activity was recorded (see the integrated trace below). (D) Graph representing the kinetics of BDNF effects on individual burst frequency (black dots) and on frequency average/min (green dots) recorded from a single preparation. Grey rectangles indicate the time window during which measurements were performed for every experiment. (E) Bar histogram depicting the mean frequency of the preBötC rhythmic activity obtained from 13 preparations; control (CTL) (white bar), BDNF (15 and 30 min; two black bars) and nerve growth factor (NGF) (100 ng/mL; grey bar; $n = 6$). BDNF induced a significant increase in the frequency of the preBötC population activity, whereas NGF had no effect (*$P < 0.05$). IO, inferior olive; XII, hypoglossal nucleus; NA, nucleus ambiguous; D, dorsal; Int, integrated; IV, fourth (ventrical); V, ventral; ns, not significant.

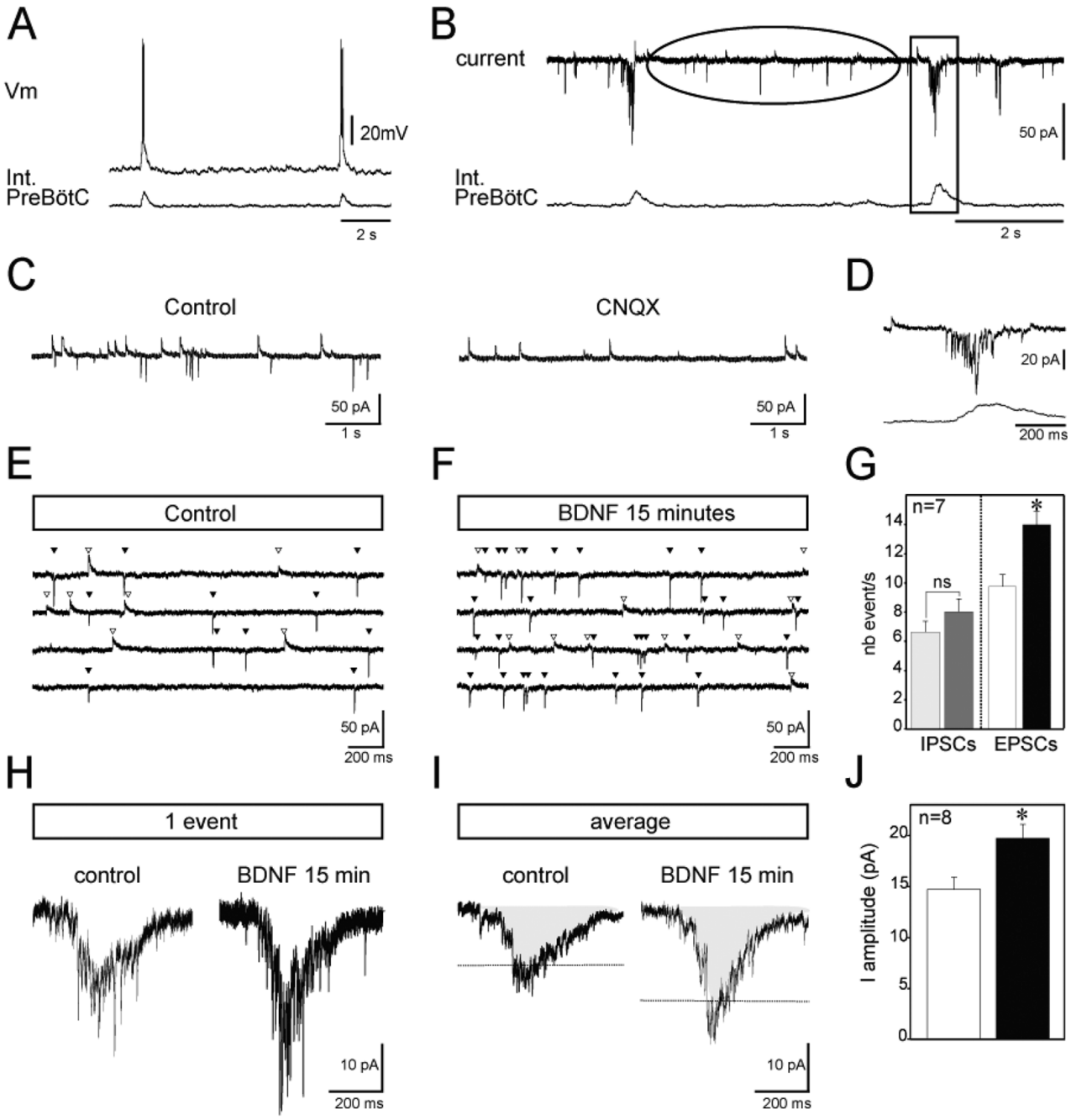

Fig. 2.

BDNF enhances the activity of glutamatergic neurons in the fetal preBötC network. Intracellular recordings (top traces) from a rhythmic preBötC neuron in current-clamp (A) and voltage-clamp (B) mode recorded simultaneously with integrated population activity (bottom traces) under control conditions. The ellipse in B indicates the period between inspiratory bursts, represented at an extended time scale for a different neuron in C. Note that the application of CNQX blocks all excitatory glutamatergic events (right panel in C). The rectangle in B highlights one inspiratory burst, represented at an extended time scale in (D). Current traces recorded between inspiratory bursts at a holding potential of −50 mV are shown in control (E) and in the presence of BDNF (F). The four traces illustrated correspond to four

samples obtained from the same neuron before and after BDNF application. White triangles indicate outward chloride-mediated synaptic currents and black triangles indicate inward glutamate-mediated synaptic currents. (G) Graph representing the mean number of inhibitory (IPSCs) and excitatory (EPSCs) events/s obtained from seven neurons in control conditions (light grey and white bars, respectively) and after BDNF treatment (dark grey and black bars, respectively). Synaptic glutamatergic drive (single event in H and average of 10 events in I) recorded from a fetal rhythmic neuron during a burst of population activity in control conditions (left panels in H and I) and after 15 min exposure to 100 ng/mL BDNF (right panels in H and I). Dashed lines indicating amplitude of the mean in the two conditions illustrate the potentiation of synaptic drive observed in the presence of BDNF. (J) Graph depicting the mean amplitude of the synaptic envelope obtained from eight neurons in control conditions (white bar) and after BDNF treatment (black bar). Int, integrated; nb, number; Vm, voltage. *$P < 0.05$.

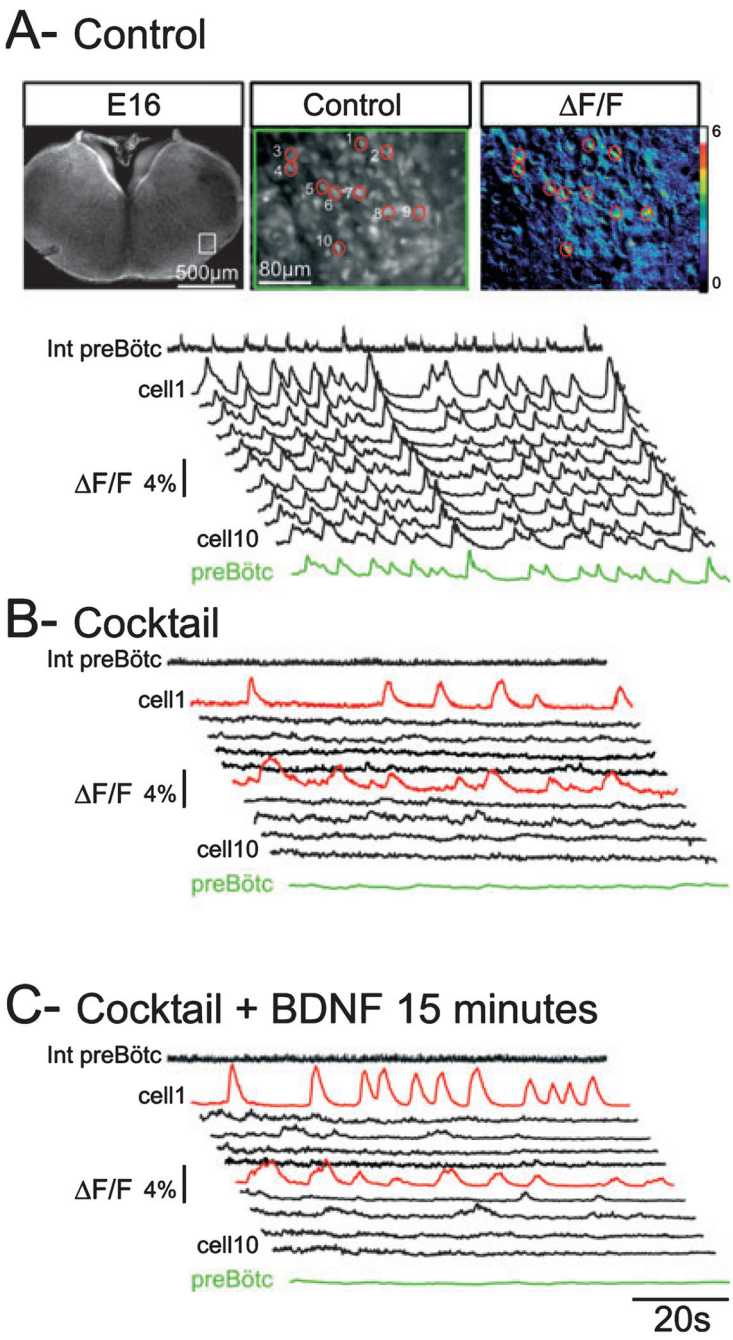

Fig. 3.

BDNF modulates the frequency activity of isolated bursting neurons. (A) Top: Fluorescent images of an E16.5 transverse medullary slice taken at low (left) and high (middle) magnification following loading with the calcium indicator Calcium Green 1-AM. Note the recording electrode positioned at the surface of the slice in the preBötC region. The white rectangle delimits the area that contains rhythmic neurons and is shown at higher magnification in the middle panel with each of the cells numbered 1–10. An example of calcium transients visualized in these cells is shown in the right panel as relative changes in fluorescence (ΔF/F). The traces in A–C display the calcium transients recorded from neurons 1–10 in control conditions (A), blocker cocktail (20 μM CNQX, 50 μM AP5, 10 μM bicuculline, 5 μM

strychnine and 50 μM carbenoxolone) (B) and blocker cocktail plus 100 ng/mL BDNF for 15 min (C). Calcium changes occurring in the preBötC area are shown in the green trace (preBötC) and electrical activity recorded in the contralateral preBötC is represented as the integrated trace (Int preBötC). In cocktail, population activity ceases (flat green trace and flat integrated recording) and synchronized calcium events disappear. The red traces highlight two neurons exhibiting endogenous bursting properties, neurons that remain rhythmically active after intra-network connectivity blockade. In the presence of BDNF the bursting frequency of these neurons increases (compare the red traces in B and C).

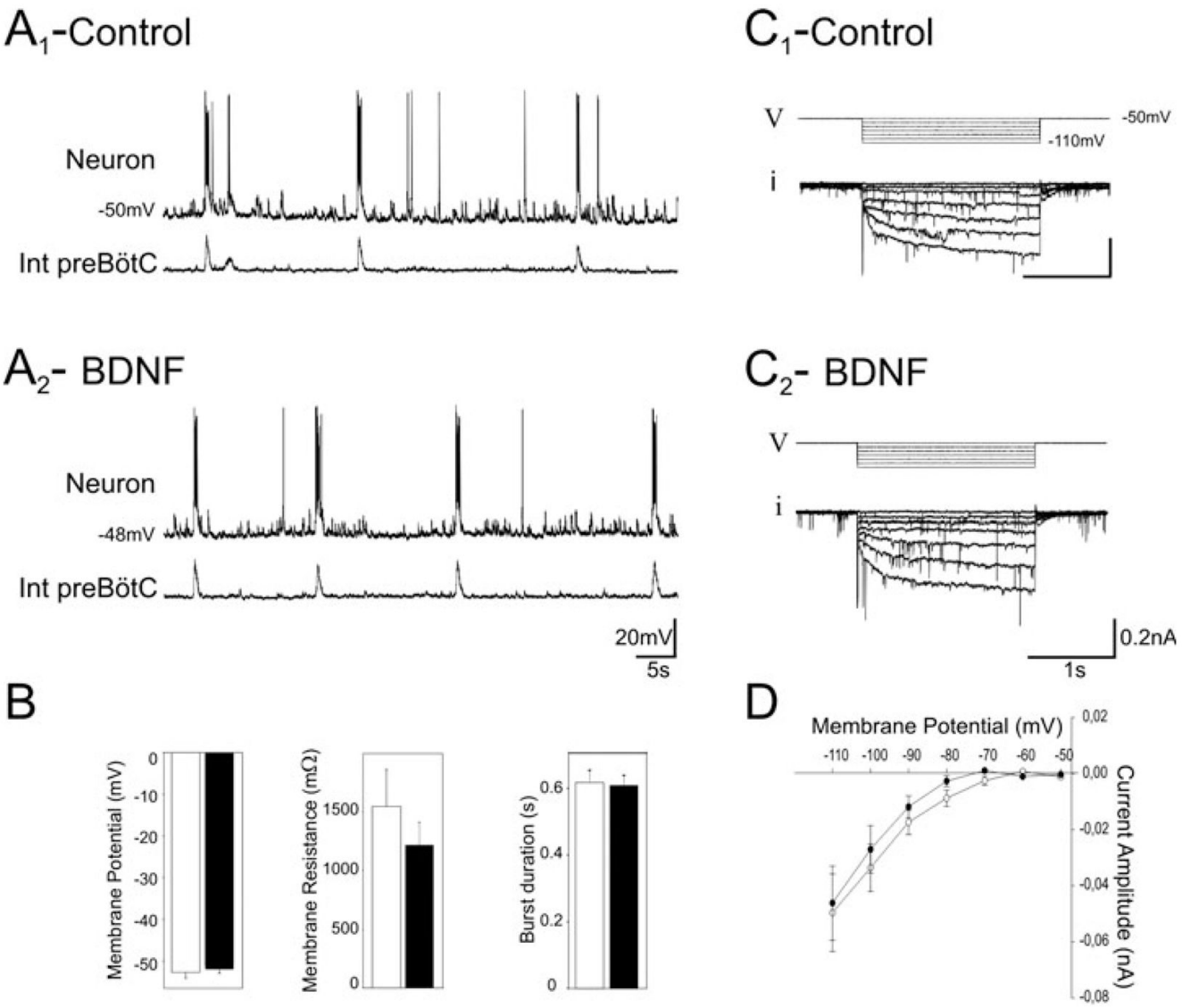

Fig. 4.

Membrane properties of inspiratory follower neurons are not affected by BDNF. (A) Intracellular recording from a rhythmic preBötC neuron (top traces) recorded simultaneously with integrated population activity (bottom traces) in control conditions (A_1) and after 15 min exposure to 100 ng/mL BDNF (A_2). (B) Bar histograms showing the mean values for membrane potential, membrane resistance and burst duration in control conditions (white bars) and in the presence of 100 ng/mL BDNF (black bars) obtained for eight neurons. Voltage stimulation protocol (V) used to evoke the Ih current (i) in control conditions (C_1) and after 15 min exposure to BDNF (C_2). (D) Graph of the Ih current amplitude vs. voltage. Mean curves were obtained from seven neurons and evoked currents were measured in control conditions (open circles) and after 15 min in the presence of 100 ng/mL BDNF (black circles). BDNF had no significant effect on any of the membrane properties tested. Int, integrated.

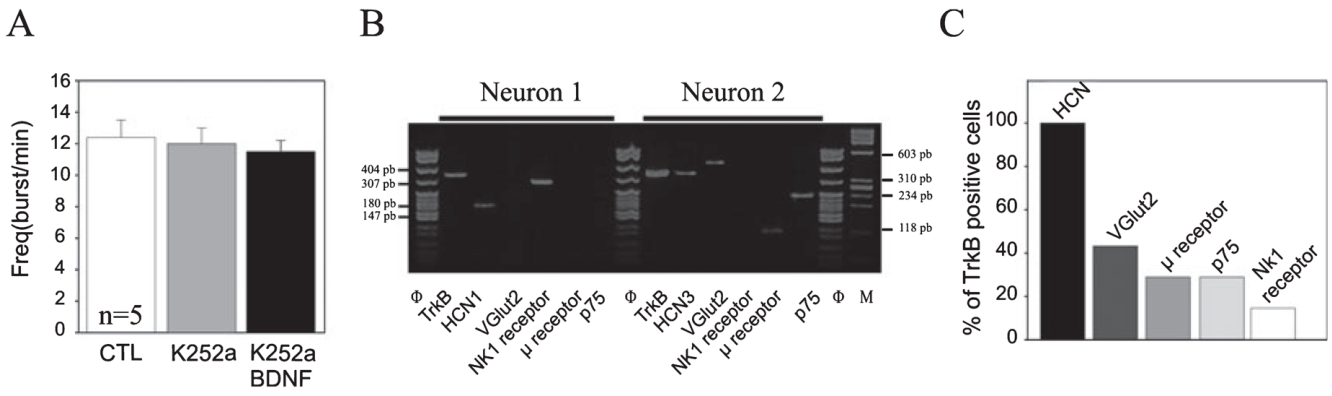

Fig. 5.

Evidence that TrkB signalling mediates BDNF regulation of fetal preBötC neuron activity. (A) Bar histograms showing the mean firing frequency of preBötC neurons (n = 5; extracellular activity from five preparations) in control (CTL) conditions (white bars), in the presence of 200 nM K252a for 1 h (light grey bar) and in the presence of 200 nM K252a plus 100 ng/mL BDNF for 15 min (black bar) following 1 h pretreatment with the tyrosine kinase inhibitor alone. In contrast to the increase in frequency observed in response to BDNF alone (Fig. 1), BDNF had no effect in the presence of K252a, consistent with a requirement for tyrosine kinase activation. (B) Agarose gel analysis of reverse transcription-PCR products amplified from two different rhythmic neurons. Φ and M correspond to molecular weight markers (indicated on the left and right of the gel). (C) Bar graph representing the proportion of TrkB-positive neurons expressing other markers, including HCNs, VGlut2, μ receptor, p75 receptor and NK1R.

Table 1

Sequence of the primers used for the first PCR in the single-cell multiplex reverse transcription-PCR protocol

	First primer pair				
	Sense PCR primers		Antisense PCR primers		
Gene	Position	Sequence	Position	Sequence	PCR product
TrkB	916–935	ACTGTGAGAGGCAACCCCAA	1327–1346	ATCACCAGCAGGCAGAATCC	431
p75	151–170	GGAGCCAACCAGACCGTGTG	410–431	TCTGGGCACTCTTCACACACTG	280
BDNF	370–389	ATGTCTATGAGGGTTCGGCG	606–625	GCGAGTTCCAGTGCCTTTTG	256
VGlut2	316–335	CGCGGAGGCAAAGTTATCAA	805–828	TCTGTAATGGTAGGATGCTTTGC	513
NK1R	34–53	TTCCCCAACACCTCCACCAA	455–474	AGCCAGGACCCAGATGACAA	441
Mu-R	75–94	ACCTGGCTCCTGGCTCAACT	290–310	TGGTGGCAGTCTTCATTTTGG	236
HCN1	1642–1663	TGTCGTCTTTACTCCCTTTCGG	1956–1975	CGGTGTAGACTGGCGGAGAT	334
HCN2	1698–1718	CAAGGGCAACAAGGAGATGAA	2056–2073	TGGCGGTGGTGGGAAGAG	376
HCN3	1530–1549	TTGTCGCCTCTACTCGCTCA	1902–1921	GGAGGGTGGCTGGAGAATCA	392
HCN4	24–43	CCGCTATCAAAGTGGAGGGA	265–284	TCAGCAACAGCATCGTCAGG	261
Intron	8–27	CTGTCCCCCTTACGAATCCC	228–247	CCAGCACCAGGGATAGAGCC	220

The primers are designed from 5′ to 3′. Position 1 corresponds to the ATG codon.

Table 2

Sequence of the primers used for the second PCR in the single-cell multiplex reverse transcription-PCR protocol

	Second primer pair				
	Sense PCR primers		Antisense PCR primers		
Gene	Position	Sequence	Position	Sequence	PCR product
TrkB	941–962	CGCTTCAGTGGTTCTACAATGG	1265–1284	CTCCCGATTGCTTTGGTCAG	344
p75	161–180	AGACCGTGTGTGAACCCTGC	364–381	GAGTCCTGAGCCCACCCC	221
BDNF	445–464	TGGGTCACAGCGGCAGATAA	575–595	TGCAGCCTTCCTTGGTGTAAC	151
VGlut2	362–379	CCGAGACCGTGGGGATGA	773–796	CATAAGACACCAGAAGCCAGAACA	435
NK1R	123–142	CATCGTGGTGACTTCCGTGG	397–416	TGAAGAGGGTGGATGATGGC	294
Mu-R	196–216	GTCACAGCCATCACCATCATG	287–310	TGGTGGCAGTCTTCATTTTGGTAT	115
HCN1	1711–1734	GCCTTTGAGACAGTTGCTATTGAC	1872–1895	TGAGGATAGTTGATTGGAGGGATA	185
HCN2	1830–1849	TTTCAACGAGGTGCTGGAGG	1968–1987	TGGCATTCTCCTGGTTGTTG	158
HCN3	1564–1583	AATGCGGTGCTTGAGGAGTT	1885–1902	AGGGGAGAGGGGCAGAGG	339
HCN4	24–43	CCGCTATCAAAGTGGAGGGA	254–275	GCATCGTCAGGTCCCAGTAAAA	252
Intron	16–35	CTTACGAATCCCCCAGCCTT	178–197	TTGAAAGCCAGGGAGGAACT	182

The primers are designed from 5′ to 3′. Position 1 corresponds to the ATG codon.